Anisotropic Laplacian Growths: From Diffusion-Limited Aggregates to Dendritic Fractals

A. Arneodo,[(1)] F. Argoul,[(1)] Y. Couder,[(2)] and M. Rabaud[(2)]

[(1)]*Centre de Recherche Paul Pascal, Avenue Schweitzer, 33600 Pessac, France*

[(2)]*Laboratoire de Physique Statistique, Ecole Normale Supérieure, 24 Rue Lhomond, 75231 Paris CEDEX 05, France*

(Received 15 January 1991)

The statistical properties of anisotropic diffusion-limited aggregates (DLA) grown in a strip are investigated. The mean shape of these aggregates being related to the corresponding smooth Saffman-Taylor solutions, a finite-size scaling analysis is applied. This scaling description shows that the anisotropy-induced crossover from isotropic DLA clusters ($D_F = \frac{5}{3}$) to dendritic fractals ($D_F = \frac{3}{2}$) is actually contained in the continuous shape transition of the stable solution, from isotropic fingers of relative width $\lambda = 0.5$ to $\lambda = 0$ needlelike fingers.

PACS numbers: 68.70.+w, 47.20.Hw, 61.50.Cj

Fractal growth is obtained in various Laplacian and diffusion-controlled systems;[1] the overall aspect of the aggregate and its fractal dimension depend upon the isotropy or anisotropy of the system. Despite many experimental[2] and numerical[3-5] efforts, there is still little understanding of the anisotropy-induced transition from isotropic to anisotropic fractal growth. The aim of the present Letter is to provide a scaling description of this morphological transition. Here, the reference system exhibiting Laplacian or diffusion-controlled growth will be viscous fingering,[6] dendritic growth,[7] and diffusion-limited aggregation[8] (DLA). Very generally, the first two systems are unstable at a length scale l_c which is of an order of magnitude given by the linear stability analysis of a planar front. For DLA, the small scale is due to the grid mesh size. An important factor for the growth is the cell geometry. A linear channel of width W was originally introduced by Saffman and Taylor[6] (ST) for viscous fingering. In this geometry, smooth fingers are observed for moderate values of the ratio l_c/W ($> \frac{1}{8}$) and fractal structures for small values of this ratio.

In the case of smooth fingers, a family of analytical solutions parametrized by their relative width λ was found in the absence of surface tension.[6] Two possible selections are observed. Normal fingers[6] (isotropic case) tend to occupy half of the channel width ($\lambda = 0.5$). Anomalous fingers[9] (anisotropic case) have a radius of curvature at the tip scaled on l_c so that with decreasing l_c/W, $\lambda \to 0$. There is a crossover between these two situations which depends upon the strength of the anisotropy. For fractal patterns, we have shown previously[10,11] that in all cases (viscous fingering, dendritic growth, and DLA) it was possible to define a mean profile by averaging repeated runs of the same experiment. The surprising result is that the average profiles have the shape and the selection of the stable solutions, thus undergoing a similar crossover when anisotropy is introduced. In this paper, we carry out a finite-size scaling analysis showing how the dependence of the fractal properties on anisotropy is related to the selected smooth solutions.

Along the line of our previous analysis[11] we will concentrate on noise-reduced DLA clusters grown on a square lattice in a strip between two reflecting walls, the lattice being parallel to the cell axis. We use a classical noise-reducing technique[4] where a particle is added to the cluster only when a number m of arrivals has been recorded. For $m = 1$, we recover the ordinary DLA model[8] [Fig. 1(a)]. When m is increased, the axis of the square lattice becomes the preferential direction of growth and the DLA clusters are progressively transformed into dendritic fractal patterns [Fig. 1(b)]. In a given strip of width W, we grow N aggregates with the same number M of particles. M is chosen large enough so that the characteristic size of the aggregate along the growth axis Ox is much larger than W. We then count for each point of the grid how many times it has been occupied by a particle of an aggregate. This number, divided by N, gives $r(x,y)$, the mean occupancy of this point.

The histogram of mean occupancy along the growth axis is found constant in the inactive region of interest, as imposed by the cell translational invariance.[10,11] Across the cell, all transverse occupancy profiles have a maximum $r_{\max}$ at the center ($y = 0$) and decrease to zero at the walls ($y = \pm W/2$). For $m = 1$, the transverse profile is remarkably well fitted by $r(x,y) = r_{\max} \times \cos^2(\pi y/W)$ [Fig. 2(a)]. For $m > 1$, the profile shrinks [Fig. 2(b)] and there is a wide gap on each edge where $r = 0$; in fact, the larger m, the narrower the transverse occupancy profile. The mean width of the occupancy probability distribution is found by determining the points $y_m^{\pm}$ on each side of the cell's axis which satisfy[11]

$$y_m^{\pm}(x) = \frac{1}{r_{\max}} \int_0^{\pm W/2} r(x,y)\, dy . \qquad (1)$$

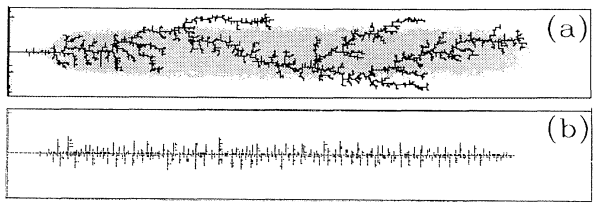

FIG. 1. (a) A DLA cluster with $m = 1$ grown in a strip of width $W = 64$; the shaded region corresponds to the points of the strip with mean occupancy $r > r(y_m^{\pm})$ as computed with 250 aggregates. (b) A noise-reduced DLA cluster with $m = 8$.

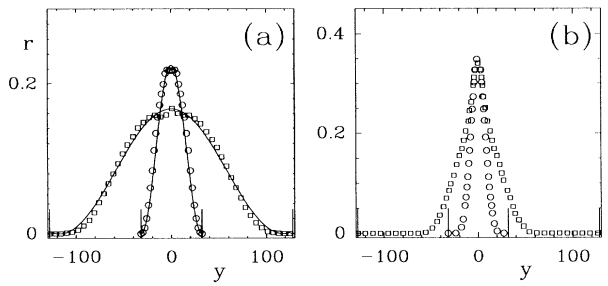

FIG. 2. Histograms of the mean transverse occupancy across a strip of width $W=64$ (○) and 256 (□) for 250 noise-reduced DLA clusters. (a) *Isotropic growth*: $m=1$, the solid lines correspond to a fit by $r(y)=r_{\max}\cos^2(\pi y/W)$. (b) *Anisotropic growth*: $m=4$.

The region of large occupancy is then defined by selecting only the points in the cell such that $r(x,y)\geq r(y_m^{\pm})$ ($y_m^{\pm}$ being independent of x in the inactive region). As shown in Fig. 1(a), the limit of this region is well fitted[10,11] by the ST solution of relative width $\lambda=(y_m^+-y_m^-)/W$. For $m=1$, we recover the $\lambda=0.5$ ST finger as the mean profile of unstable fractal DLA aggregates.[10] Unlike the isotropic case,[12] for a given $m>1$, the relative width of the region of large occupancy depends on the width of the cell. As illustrated in Fig. 3(a), when increasing W, λ decreases to zero at a rate which is m dependent. This crossover behavior indicates that the effective anisotropy in the growth process can be controlled by either tuning the noise-reducing parameter m or changing the width W of the strip through the scaling variable $m^{\nu}W$. A good fit of all the data is obtained by choosing $\nu=\frac{3}{2}$. In Fig. 3(b) we show that the dependence of λ on m and W can be represented by the finite-size scaling form

$$\lambda=\Lambda(1/m^{3/2}W)\,, \tag{2}$$

where the universal crossover scaling function $\Lambda(u)$ behaves as $\Lambda(u)\simeq\frac{1}{2}$ for $u\gg u_c$ and $\Lambda(u)\sim u^{1/2}$ for $u\ll u_c$, where u_c is a finite critical value.

For anomalous fingers, the relevant quantity is the radius of curvature at the tip:[6] $\rho=\lambda^2W/\pi(1-\lambda)$. It was shown previously[11] that the ST mean profile of noise-reduced aggregates was also selected by its ρ. In Fig. 3(c) we present the radius of curvature at the tip of the mean occupancy profile of noise-reduced DLA clusters versus W, for different values of m. For $m=1$, the observation that $\lambda=\frac{1}{2}$ implies that ρ scales linearly on W ($\rho=W/2\pi$). Very much like the stable compact fingers, the fractal patterns are selected by the largest length scale of the system,[10] i.e., W. For a given $m>1$, ρ increases initially with W up to some critical width W_c, which depends on m, where it reaches a constant value. For anisotropic DLA clusters, the width of large occupancy is now selected by its radius of curvature at the tip.[11] This is precisely the selection mechanism of stable anomalous viscous fingers and parabolic needle crystals. In Fig. 3(d) we show that ρ satisfies the following finite-

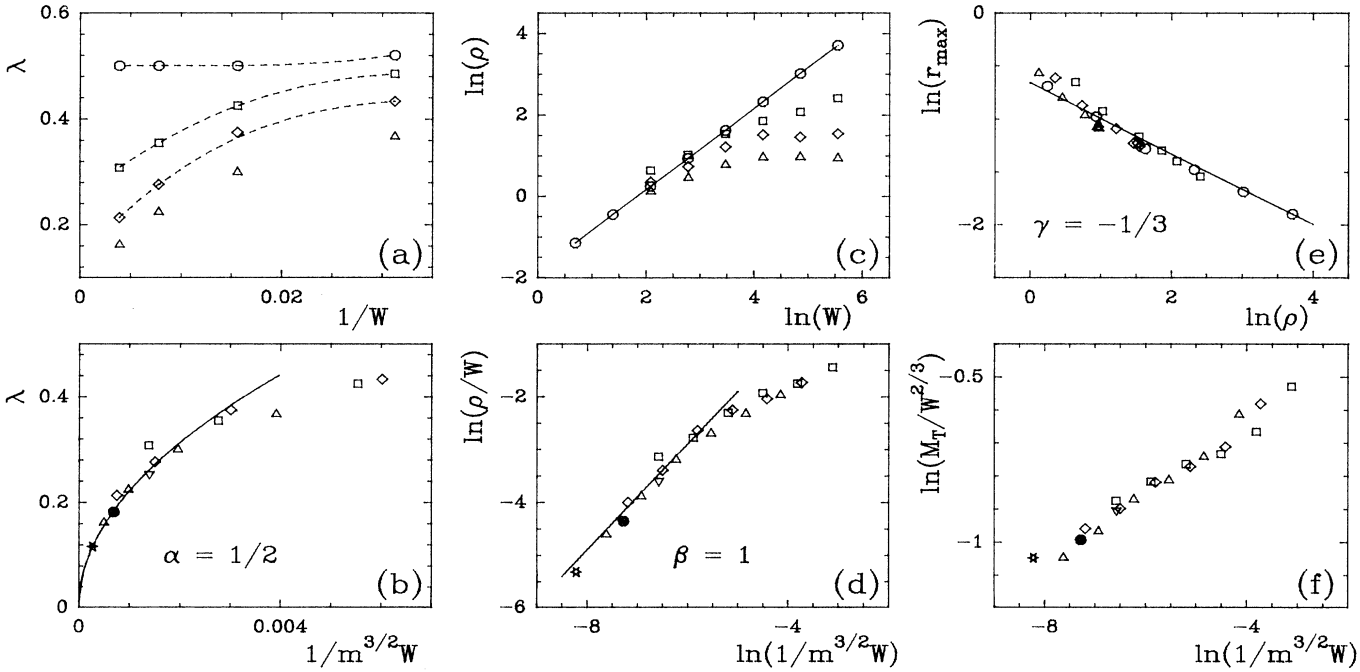

FIG. 3. Characteristics of the mean occupancy profile of 250 noise-reduced DLA clusters grown in a strip of width W. The symbols correspond to different values of $m=1$ (○), 2 (□), 3 (◇), 4 (△), 5 (▽), 8 (●), and 15 (*). (a) λ vs $1/W$. (b) λ vs $1/m^{3/2}W$; the solid line corresponds to the scaling behavior $\Lambda(u)\sim u^{\alpha}$ with $\alpha=\frac{1}{2}$ [Eq. (2)]. (c) $\ln\rho$ vs $\ln W$. (d) $\ln\rho/W$ vs $\ln(1/m^{3/2}W)$; the solid line corresponds to the scaling behavior $\mathcal{R}(u)\sim u^{\beta}$ and $\beta=1$ [Eq. (3)]. (e) $\ln r_{\max}$ vs $\ln\rho$; the solid line corresponds to the power-law behavior $r_{\max}\sim\rho^{\gamma}$ with $\gamma=-\frac{1}{3}$. (f) $\ln(M_T/W^{2/3})$ vs $\ln(1/m^{3/2}W)$ [Eq. (4)].

size scaling behavior

$$\rho = W\mathcal{R}(1/m^{3/2}W), \tag{3}$$

where the scaling function $\mathcal{R}(u)$ has the properties $\mathcal{R}(u) \simeq 1/2\pi$ for $u \gg u_c$ (isotropic growth) and $\mathcal{R}(u) \sim u$ for $u \ll u_c$ (anisotropic growth). For large effective anisotropy ($m^{3/2}W \gg 1/u_c$), this implies that $\rho \sim m^{-3/2}$, independently of W. At large values of m, the cutoff value induced by the grid mesh size is reached and the aggregates, like dendrites, are compact at the tip. This morphological evolution manifests itself in the transverse profile by a systematic increase of $r_{\max}$ towards 1 due to the anisotropy-induced stabilization of the tip of the aggregate against tip splitting. Although there is *a priori* no surface tension in the problem, the noise-reducing parameter m for DLA clusters grown on a square lattice[10,11] ($\rho \sim m^{-3/2}$) can thus be seen as playing a role analogous to surface-tension anisotropy in viscous fingering and crystal growth[7,9] ($\rho \sim \epsilon^{-7/8}$, where ϵ characterizes the presence of fourfold anisotropy).

The next step in our demonstration is to show that the geometrical properties of these Laplacian fractal patterns are in turn amenable to a finite-size scaling description. From the translational invariance of the occupancy probability distribution along the growth axis, one deduces readily that the mass has a one-dimensional component in the Ox direction, $M(x) \sim x$, i.e., the longitudinal partial dimension $D_L = 1$. Obviously, the fractality of the patterns has to come from the direction perpendicular to the growth axis.[5] The computation of the area of the transverse occupancy profile (Fig. 2) as a function of the width of the strip gives the transverse partial dimension $M_T(W) \sim W^{D_T}$. From the definition [Eq. (1)] of the region of large occupancy, the area of the transverse profile is equal to the area of a step-function profile of width λW and height $r_{\max}$, i.e., $M_T(W) = r_{\max}\lambda W$. The data presented in Fig. 3(e) provide evidence for a general scaling relationship between $r_{\max}$ and ρ: $r_{\max} = f(\rho) \sim \rho^{-1/3}$. *Isotropic ($m = 1$) DLA clusters:*[12] From the observation that $\lambda = \frac{1}{2}$ or equivalently $\rho = W/2\pi$, one deduces that $r_{\max} \sim W^{-1/3}$ which yields $M_T \sim W^{2/3}$. Combining $D_T = \frac{2}{3}$ and $D_L = 1$, one gets a fractal dimension $D_F = \frac{5}{3}$ which matches perfectly the mean-field prediction[13] $D_F = (d^2+1)/(d+1)$ for diffusion-limited aggregation in dimension $d = 2$. *Anisotropic ($m > 1$) noise-reduced DLA clusters:* Along the line of our finite-size scaling analysis, one can reasonably propose the scaling ansatz

$$M_T(m,W) = W^{2/3}\mathcal{M}(1/m^{3/2}W), \tag{4}$$

where the scaling function $\mathcal{M}(u)$ behaves as $\mathcal{M}(u) \sim$ const for $u \gg u_c$ and $\mathcal{M}(u) \sim u^{\delta}$ for $u \ll u_c$. Equation (4) accounts for a crossover from $D_T = \frac{2}{3}$ (isotropic growth, $D_F = \frac{5}{3}$) to $D_T = \frac{2}{3} - \delta$ (dendritic growth, $D_F = \frac{5}{3} - \delta$) when increasing the effective anisotropy parameter $m^{3/2}W$. The data collapse predicted by Eq. (4) is numerically tested in Fig. 3(f). Although the existence of the scaling function $\mathcal{M}(u)$ is clearly revealed, the numerical results gathered in Fig. 3(f) do not provide an asymptotic estimate of the exponent δ; this would require the analysis of patterns with large m and W values far beyond our computational potential.

Fortunately, there is an analytical alternative which relies on the observation that $r_{\max} = f(\rho)$ no longer depends on W as soon as ρ does not depend on W [Figs. 3(c) and 3(e)]. From the scaling relation (3) and the results in Fig. 3(d), this happens for $Y = W/2\pi\rho \geq Y_c$, where $Y_c \simeq 3$. Let us remark that $Y = 1$ corresponds to isotropic growth, while the limit $Y \sim m^{3/2}W \to +\infty$ corresponds to the dendritic limit at large effective anisotropy. The fractal properties of noise-reduced DLA clusters are thus contained in the Y dependence of λ via $M_T(Y) \sim \lambda(Y)Y \sim Y^{D_T}$. Since $D_L = 1$, one gets $\lambda(Y) \sim Y^{D_F(Y)-2}$. But $\lambda(Y)$ is known from the expression of the radius of curvature at the tip of the analytical ST solutions:[6] $\lambda(Y) = -1/4Y + (2/Y + 1/4Y^2)^{1/2}/2$. This leads to the following differential equation for $D_F(Y)$:

$$\frac{dD_F(Y)}{dY} + \frac{D_F(Y)}{Y \ln Y} = \frac{1}{Y \ln Y}\left[1 + \frac{4Y}{1+8Y-(1+8Y)^{1/2}}\right]. \tag{5}$$

A straightforward integration yields the following analytical expression for $D_F(Y)$ ($Y > Y_c$):

$$D_F(Y) = 1 + \frac{1}{\ln Y}\left[[D_F(Y_c) - 1]\ln Y_c + \ln\frac{(1+8Y)^{1/2}-1}{(1+8Y_c)^{1/2}-1}\right], \tag{6}$$

where the constant of integration $D_F(Y_c)$ is a free parameter. In Fig. 4, we compare Eq. (6) with direct box-counting measurements of the fractal dimension of noise-reduced DLA clusters ($m = 1$–15) grown in a strip of width $W = 512$. With an adequate choice of $D_F(Y_c)$, the analytical expression (6) provides a very good fit of the experimental box-counting dimensions. Let us re-

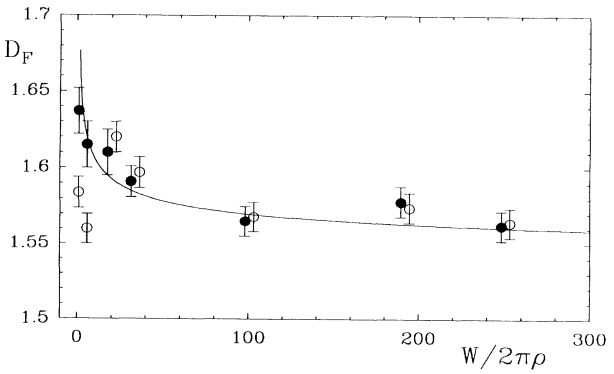

FIG. 4. Box-counting measurements of the fractal dimension D_F of noise-reduced DLA clusters grown in a strip of width $W = 512$ with values of m ranging from $m = 1$ to $m = 15$: inactive region (●), active region (○). The solid line corresponds to the analytical prediction (6) with $D_F(Y_c = 3) = 1.64$.

mark, however, that for $Y \leq Y_c$, the box-counting dimension in the active region ($D_F \simeq 1.57 \pm 0.02$) is significantly smaller than in the inactive region as already noticed in previous works.[14] Considering the limit $Y \to +\infty$ in Eq. (6) leads to the following asymptotic value for the fractal dimension of dendritic fractals: $D_F(Y) = \frac{3}{2} + O(1/\ln Y)$. The very slow logarithmic convergence to $D_F = \frac{3}{2}$ makes this limit quite inaccessible in numerical experiments; this may explain the difficulties encountered in previous studies to approach this asymptotic prediction.[1] Finally let us mention that from the relation $D_F = \frac{3}{2} = \frac{5}{3} - \delta$, one predicts the value $\delta = \frac{1}{6}$ for the power-law exponent of the scaling function $\mathcal{M}(u)$ in Eq. (4) for $u \ll u_c$.

In conclusion, the shape of the mean transverse profiles of fractal patterns grown in a strip depends on an effective anisotropy. This is in direct correspondence with a crossover known for stable smooth fingers.[15] A finite-size scaling analysis of these mean profiles thus provides a picture for the anisotropy-induced morphological transition of fractal patterns grown in Laplacian fields. It predicts the fractal dimension's dependence on the effective anisotropy (which results from both the anisotropy and the channel width). From this analysis, we obtain the two limiting values $D_F = \frac{5}{3}$ for isotropic DLA clusters and $D_F = \frac{3}{2}$ for anisotropic dendritic fractals.

We benefited from useful discussions with M. Ben Amar and V. Hakim. This work was supported by the Centre National d'Etudes Spatiales under Contract No. 90/215 and the Direction des Recherches Etudes et Techniques under Contact No. 89/196. Two of us (A.A. and F.A.) would like to acknowledge the hospitality of the Center for Nonlinear Dynamics at the University of Texas (Austin) where part of this work was done. Laboratoire de Physique Statistique, Ecole Normale Supérieure, is associated with CNRS and Universités Paris VI and Paris VII.

[1]T. Vicsek, *Fractal Growth Phenomena* (World Scientific, Singapore, 1989), and references therein.

[2]E. Ben-Jacob, R. Godbey, N. D. Goldenfeld, J. Koplik, H. Levin, T. Mueller, and L. M. Sander, Phys. Rev. Lett. **55**, 1315 (1985); V. Horvath, T. Vicsek, and J. Kertèsz, Phys. Rev. A **35**, 2353 (1987); D. Grier, E. Ben Jacob, R. Clarke, and L. M. Sander, Phys. Rev. Lett. **56**, 1264 (1986).

[3]J. Nittman and H. E. Stanley, Nature (London) **321**, 663 (1986).

[4]C. Tang, Phys. Rev. A **31**, 1977 (1985); J. Kertèsz and T. Vicsek, J. Phys. A **19**, L257 (1986); P. Meakin, J. Kertèsz, and T. Vicsek, J. Phys. A **21**, 1271 (1988).

[5]J. P. Eckmann, P. Meakin, I. Procaccia, and R. Zeitak, Phys. Rev. A **39**, 3185 (1989); Phys. Rev. Lett. **65**, 52 (1990).

[6]P. G. Saffman and G. I. Taylor, Proc. Roy. Soc. London A **245**, 312 (1958); D. Bensimon, L. P. Kadanoff, S. Liang, B. I. Shraiman, and Chao Tang, Rev. Mod. Phys. **58**, 977 (1986).

[7]J. S. Langer, in *Chance and Matter,* edited by J. Souletie, J. Vanimenus, and R. Stora (North-Holland, Amsterdam, 1987); D. A. Kessler, J. Koplik, and H. Levine, Adv. Phys. **37**, 255 (1988); P. Pelcé, *Dynamics of Curved Fronts* (Academic, Orlando, 1988).

[8]T. Witten and L. M. Sander, Phys. Rev. Lett. **47**, 1400 (1981); Phys. Rev. B **27**, 5686 (1983).

[9]M. Rabaud, Y. Couder, and N. Gérard, Phys. Rev. A **37**, 935 (1988).

[10]A. Arneodo, Y. Couder, G. Grasseau, V. Hakim, and M. Rabaud, Phys. Rev. Lett. **63**, 984 (1989).

[11]Y. Couder, F. Argoul, A. Arneodo, J. Maurer, and M. Rabaud, Phys. Rev. A **42**, 3499 (1990).

[12]Large-mass DLA clusters grown on a square lattice are known to display preferential directions of growth. The values of W considered here are relatively small so that the case $m = 1$ actually mimics isotropic growth.

[13]M. Tokuyama and K. Kawasaki, Phys. Lett. **100A**, 337 (1984); K. Honda, H. Toyoki, and M. Matsushita, J. Phys. Soc. Jpn. **55**, 707 (1986).

[14]J. Feder, E. L. Hinrischen, K. J. Maloy, and T. Jossang, Physica (Amsterdam) **38D**, 104 (1989).

[15]For smooth solutions [see Ref. 7 and A. T. Dorsey and O. Martin, Phys. Rev. A **35**, 3989 (1987)], the finger is selected by $\rho \sim \epsilon^{-7/8} l_c$. The crossovers obtained for different widths and various anisotropies would then be reconciled by using a variable $u = 1/\epsilon^{7/8} W$. However, this would be valid only in the limit of weak anisotropy. Different exponents were found in numerical investigations [D. Kessler, J. Koplik, and H. Levine, Phys. Rev. A **34**, 4980 (1986); M. Ben Amar (private communication)] for larger values of ϵ.